Identification of the Interfacial Surface in Separation of Two-Phase Multicomponent Systems

Ivan Pavlenko [1], **Oleksandr Liaposhchenko [1]**, **Vsevolod Sklabinskyi [1]**, **Vitaly Storozhenko [1]**, **Yakov Mikhajlovskiy [1]**, **Marek Ochowiak [2,*]**, **Vitalii Ivanov [1]**, **Jan Pitel [3]**, **Oleksandr Starynskyi [1]**, **Sylwia Włodarczak [2]**, **Andżelika Krupińska [2]** and **Małgorzata Markowska [2]**

[1] Sumy State University, Faculty of Technical Systems and Energy Efficient Technologies, 2 Rymskogo-Korsakova St., 40007 Sumy, Ukraine; i.pavlenko@omdm.sumdu.edu.ua (I.P.); o.liaposhchenko@pohnp.sumdu.edu.ua (O.L.); v.sklabinskyi@pohnp.sumdu.edu.ua (V.S.); info@dir.sumdu.edu.ua (V.S.); y.mykhailovskyi@pohnp.sumdu.edu.ua (Y.M.); ivanov@tmvi.sumdu.edu.ua (V.I.); oleksandr.starynskyj@ms.sumdu.edu.ua (O.S.)

[2] Poznan University of Technology, Department of Chemical Engineering and Equipment, Poznan University of Technology, 60-965 Poznan, Poland; sylwia.wlodarczak@put.poznan.pl (S.W.); andzelika.krupinska@doctorate.put.poznan.pl (A.K.); malgorzata.markowska@doctorate.put.poznan.pl (M.M.)

[3] Faculty of Manufacturing Technologies, Technical University of Kosice, 1 Bayerova St., 080 01 Presov, Slovakia; jan.pitel@tuke.sk

* Correspondence: marek.ochowiak@put.poznan.pl

Abstract: The area of the contact surface of phases is one of the main hydrodynamic indicators determining the separation and heat and mass transfer equipment calculations. Methods of evaluating this indicator in the separation of multicomponent two-phase systems were considered. It was established that the existing methods for determining the interfacial surface are empirical ones, therefore limited in their applications. Consequently, the use of the corresponding approaches is appropriate for certain technological equipment only. Due to the abovementioned reasons, the universal analytical formula for determining the interfacial surface was developed. The approach is based on both the deterministic and probabilistic mathematical models. The methodology was approved on the example of separation of two-phase systems considering the different fractional distribution of dispersed particles. It was proved that the area of the contact surface with an accuracy to a dimensionless ratio depends on the volume concentration of the dispersed phase and the volume of flow. The separate cases of evaluating the contact area ratio were considered for different laws of the fractional distribution of dispersed particles. As a result, the dependence on the identification of the abovementioned dimensionless ratio was proposed, as well as its limiting values were determined. Finally, a need for the introduction of the correction factor was substantiated and practically proved on the example of mass-transfer equipment.

Keywords: multiphase flow; separation; heat and mass transfer; probabilistic approach; fractional distribution; contact area ratio

1. Introduction

Adsorption, rectification, and separation processes are accompanied by heat and mass transfer. As known, the transfer of heat and mass derives through the surface of the phase contact, which is obtained from the surfaces of dispersed gas or liquid particles in a continuous phase. The area size of the interfacial surface is the main hydrodynamic indicator and defining characteristic for the

design of heat–mass transfer and separation equipment. This parameter is basic for calculations of technological modes of heat–mass transfer and separation processes, the dimensions and number of single contact and separation sections, and consequently the main unit dimensions. The specific interfacial surface *a* per unit volume is commonly determined depending on the average diameter of the dispersed particles d_p and gas volume fraction φ as $a = 6\varphi/d_p$, where coefficient 6 corresponds with the case of particles of the equal diameters. However, despite the wide use of this expression, there is no theoretical foundation to evaluate this coefficient for different distribution laws of particle size.

The specific interfacial surfaces for individual cases are also possible to determine using other quantities and their conversion. For example, the above equation can be used for calculation of the specific contact surface per unit area of a tray or the contact surface in bubble absorbers with mechanical mixing.

Herewith, the calculation of the interfacial area is difficult due to the impossibility of accurately determining the diameter of an individual dispersed particle, their quantity per unit volume, and the heterogeneous structure of the interfacial layer. It is almost impossible to calculate the exact value of the droplet diameter since their shape and size constantly change as a result of a breakup or merging with another drop. It takes place under the action of gravity, buoyancy, surface tension, the resistance of the continuous phase, etc. It should be noted that the mechanisms of the formation of dispersed particles in the oil/gas separation equipment are natural in contrast to mass transfer equipment. For example, single-phase flows are introduced into an absorber and after passing through dispersant or contact elements bubbles and droplets are formed. On the other hand, gas or liquid flow with a wide range of dispersed phase is introduced into the separators. The diameter of the dispersed particles in the separation equipment volume is a function of the three coordinates and time because the drop passes through devices for separation and coalescence from the moment of their formation or entry into the equipment by the time of transition to another phase (condensation, evaporation) or merging with the primary phase. Doubtless, determining the droplet diameter for separators is a more complex task and requires considering the fractional distribution of dispersed particles, unlike mass transfer equipment.

Determination of the interfacial surface in mass transfer equipment is provided by choosing from a significant number of experimental methods, which do not determine actual surface with considering the different activities of dispersed particles but by some of its averaged value—the effective surface. These methods are divided into three groups according to their intended purpose. The first group includes methods applied to equipment with the fixed interfacial surface, the second group includes methods for bubbling machines and in some cases for spraying equipment, the third group is chemical methods. The last group is the most universal for devices of all types. What is more, analytical or mathematical methods for determining the area of the interfacial surface were not found. Besides, many types of research are devoted to the processes of dispersed bubbles or drop formation, the laws of their movement, and the calculation of the diameter. Such researchers as Anshtein, Ditnersky, and Gelperin considered processes which occur in the absorption and fractionating equipment. They noted that for the formation of dispersed particles, their sizes depend on the liquid/gas outflow mode (free, chain) and dispersion mode (drip, wave, saw) which is implemented by various devices. Bystryi and Kutepov paid attention to the motion modes of both a separate dispersed particle in a continuous medium and two separate phases inside the same equipment. For example, individual bubble movement is described at different values of the Reynolds criterion. In addition, the resistance coefficients of the particle movement are calculated by sphericity of its shape. In addition, models of the multiphase flow's movement are considered by both the abovementioned researchers: the homogeneous flow model, the separated flow, and the drifting flow. The structures of liquid–gas systems (e.g., bubble, drop) are also considered. The motion characteristics of dispersed particles are determined by these models.

Therefore, the aim of the research is in creating analytical solutions for determining the interfacial surface during the separation of two-phase multicomponent systems considering the fractional distribution of dispersed particles as an important feature for ensuring the reliable mathematical modeling, numerical simulation, and designing the separation equipment.

2. Literature Review

High requirements of output product quality are presented to modern separation and mass transfer equipment that is why their design requires reliable calculation methods as noted above. Therefore, a significant amount of research is aimed at determining the basic hydrodynamic characteristics of both individual devices and separation, contact devices, developing and improving new methods for separating multi-component systems, and studying the behavior and characteristics of dispersed particles in the continuous phase. In turn, these studies allow for more accurately describing and understanding separation and mass transfer mechanisms with considering secondary factors, in addition to an increase in their efficiency and intensity, at the same time developing new or improve existing algorithms for calculating process equipment.

Most researchers determine the effective interfacial surface area by experimental studies. In [1], the effective mass transfer area in a turbulent contact absorber has been determined using chemical absorption of CO_2 in an aqueous solution of NaOH and it has been established that the effective phase contact area is 3–6 times larger than the exact geometric area of the solid filler. Similar studies have been performed to determine the effective mass transfer area for unstructured filler (Raschig metal rings, nominal diameter 20–70 mm) using chemical absorption [2]. In [3–7], the effective surface area of the rotating filtering packing section has been determined. The influence of the packing radial thickness, the rotational speed, and the liquid and gas volume flow rate on the effective interface has been also studied. The effective surface of phase contact is also determined for porous media [8] by using the gas-absorption/chemical-reaction (GACR) method, which is also used to estimate the gas–liquid interfacial space in the reaction system. In [9–12], synchrotron X-ray microtomography has been used for obtaining solid/liquid phases three-dimensional images with high resolution in structured nozzle columns. The obtained images have been processed to obtain quantitative characteristics of the distribution area of the organic liquid/water and the gas phase/water for calculating of the organic liquid droplets size. A comparison of methods for estimation of the interfacial surface in porous media is carried out in [10,12]. The interfacial area between mutually insoluble liquids has been experimentally calculated using high-resolution microtomographic imaging and interfacial partitioning tracer tests (IPTT). It should be noted that most studies that aimed at the determination of the interfacial surface are experimental. This is caused by the absence of the universal analytical or mathematical methods of calculating the interfacial surface area for separation and heat transfer processes, which could be used for easier development of the innovative separation equipment and solving the problem of the optimal layout at the initial design stages. New methods of separating multicomponent systems have been created for example separation in a vortex flow [13], separation under the action of a magnetic field [14], inertia-filtrating, gas dynamic, vibration-inertial, and acoustic separation. The ways for intensification of the operating process [15,16], and methodology of numerical simulations of heat and mass exchange processes, as well as approaches to improve parameters for the corresponding multi-functional oil–gas separators and shell-and-tube heat exchangers, are presented in [17,18].

Attention should be paid to the rapid development of superoleophobic/superoleophilic, superhydrophilic/superhydrophobic surfaces [19–23] and membranes [24–27] as well as energy-efficient modular separation devices, which are used for separation of oil–water emulsions and gas–liquid mixtures. Additionally, the appliance of inertial gas-dynamic separation of gas-dispersion flows in the curvilinear convergent–divergent channels [28] to improve the reliability of compressor equipment is presented in [29].

Recently, the concepts of the hydrodynamic characteristics of dispersed particles in the continuous mobile phase have also been expanded. The phenomena of coalescence of dispersed particles, their transition into a continuous phase, and behavior on hydrophobic surfaces have been studied [30–32]. The practical significance of the research in this field is highlighted in previous studies by the need to develop oil–gas cleaning equipment [33], to design spray towers [34], and to improve the inertia-filtering separation process [35,36] with a highly developed interfacial surface.

Finally, considering the abovementioned studies, the aim of the research is to create a mathematical model to determine the interfacial surface for the separation of multicomponent systems. To achieve this goal, the following objectives were formulated: description of the discrete model for determining the interfacial surface; creation of a probabilistic model of the interfacial surface; determination of a range for variation coefficients of the proposed models for the cases of different distribution laws; evaluating ranges of the variation coefficient for the developed mathematical model; evaluating a range of the correction factor to clarify the general dependence for the specific interfacial surface; proving the reliability of the proposed approach on the example of calculation of the interfacial surface in the gas–liquid reactor.

3. Research Methodology

3.1. The Deterministic Approach

According to the deterministic approach, for the development of a mathematical model for determining the surface of heat and mass transfer, a two-phase multi-component system is considered. This hydromechanical system consists of a limited set of spherical particles with radius R_i ($i = 1, 2, \ldots, N$) of the total amount N, in a limited volume V of a medium.

The total volume of the disperse phase is determined by the following dependency:

$$V_0 = \frac{4\pi N}{3} \sum_{j=1}^{P} n_j R_j^3, \tag{1}$$

where $j = 1, 2, \ldots, P$—index of the set of particles with the same size R_j; P—number of dispersed compositions; n_j—frequency of dispersed particles in the set j determined as a ratio of their number N_j to the total number N of particles in the hydromechanical system (Figure 1):

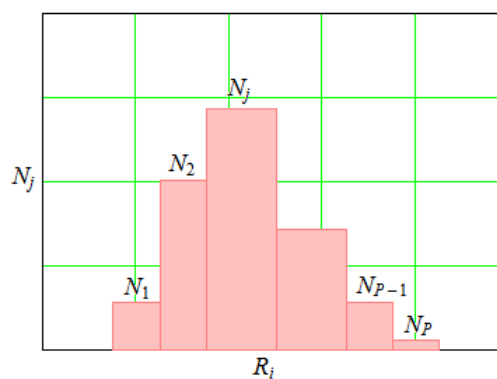$$n_j = \frac{N_j}{\sum_{j=1}^{P} N_j} = \frac{N_j}{N} \tag{2}$$

Figure 1. The distribution of a number N_j of dispersed particles by their size R_j.

In this case, the obligatory identity must be fulfilled:

$$\sum_{j=1}^{P} n_j = 1. \tag{3}$$

The interfacial surface is determined as a sum of areas for all particles in the hydromechanical system:

$$S = 4\pi N \sum_{j=1}^{P} n_j R_j^2. \tag{4}$$

The volume concentration of the dispersed phase determined as a ratio of the total volume of particles to the total volume of the medium:

$$c = \frac{V_0}{V}, \tag{5}$$

can be rewritten considering the dependence (1) in the following form:

$$c = \frac{4\pi N}{3V} \sum_{j=1}^{P} n_j R_i^3. \tag{6}$$

Since the total interfacial area is proportional to the square of particle radiuses, and the total volume of the disperse phase is proportional to their cube, it is expedient to introduce the contact area ratio as follows:

$$\alpha = \frac{S}{V_0^{2/3} N^{1/3}}, \tag{7}$$

which takes the following form considering the dependencies (4) and (6):

$$\alpha = 4.84 \frac{\sum_{j=1}^{P} n_j R_j^2}{\left(\sum_{j=1}^{P} n_j R_j^3\right)^{2/3}}, \tag{8}$$

where the value $\alpha = \sqrt[3]{36\pi} \approx 4.84$ is equal to the contact area ratio for a single particle.

It should be noted that, in general, the dimensionless ratio α depends on the distribution law of dispersed particle in terms of its size. Additionally, it can be evaluated empirically using dimensionless criteria [37]. Moreover, the introduction of this ratio allows one to obtain a universal dependence for determining the total interfacial area in the separation of two-phase multicomponent systems with joint heat and mass transfer. In this case, considering the dependence (5), it can be calculated from Equation (7):

$$S = \alpha N^{1/3} V_0^{2/3}. \tag{9}$$

Thus, the total interfacial area depends on the volume of a medium and on the concentration of the dispersed phase. In this case, it does not depend directly on particle size, but only on the law of their distribution that determines the contact area ratio α.

3.2. The Probabilistic Approach

The abovementioned deterministic approach for the determination of the total area of the interfacial surface is limited by the discrete feature of the distribution of particles in terms of radii/diameters, and by their total amount. This disadvantage is eliminated by considering the relatively infinite set of particles with the continuous distribution law for their size. In this case, the density of the probabilistic distribution of particles is introduced (Figure 2):

$$p(R) = \lim_{P \to \infty} \left(n_j\right), \tag{10}$$

which corresponds to the following obligatory condition:

$$\int_{R_{min}}^{R_{max}} p(R)dR = 1 \tag{11}$$

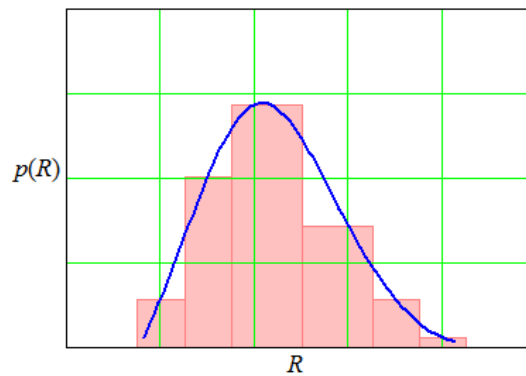for the entire range $[R_{min}, R_{max}]$ of dispersed particle sizes.

Figure 2. The distribution density of dispersed particles.

Additionally, the sum of the discrete values for the contact surfaces is replaced by a definite integral, and the dependence (4) takes the following form:

$$S = 4\pi N \int_{R_{min}}^{R_{max}} R^2 p(R)dR. \tag{12}$$

Similarly, the dependence (6) for the volume concentration is as follows:

$$c = \frac{4\pi N}{3V} \int_{R_{min}}^{R_{max}} R^3 p(R)dR. \tag{13}$$

In this case, the contact area ratio (8) is determined by the formula:

$$\alpha = 4.84 \frac{\int_{R_{min}}^{R_{max}} R^2 p(R)dR}{\left[\int_{R_{min}}^{R_{max}} R^3 p(R)dR\right]^{2/3}} \tag{14}$$

and the universal dependence (9) remains unchanged for the determination of the total contact area of phases in the separation of two-phase multicomponent systems with the joint heat and mass transfer.

Finally, the application of the probabilistic approach for developing a continuum mathematical model of determining the interfacial surface is reduced to identifying the ratio α as a function of parameters of the distribution law for dispersed particles.

4. Results

4.1. Uniform Distribution Law

Considering the uniform distribution of the continuous, randomly variable, dispersed particle size, the probability density is determined by the following formula:

$$p(R) = \frac{1}{R_{max} - R_{min}} = const. \tag{15}$$

Substitution of this dependence to Equation (14) allows one to obtain the analytical dependence for determining the contact area ratio (Figure 3):

$$\alpha = 4.06 \frac{1 + \frac{R_{min}}{R_{max}} + \left(\frac{R_{min}}{R_{max}}\right)^2}{\left(1 + \frac{R_{min}}{R_{max}}\right)^{2/3}\left[1 + \left(\frac{R_{min}}{R_{max}}\right)^2\right]^{2/3}}. \tag{16}$$
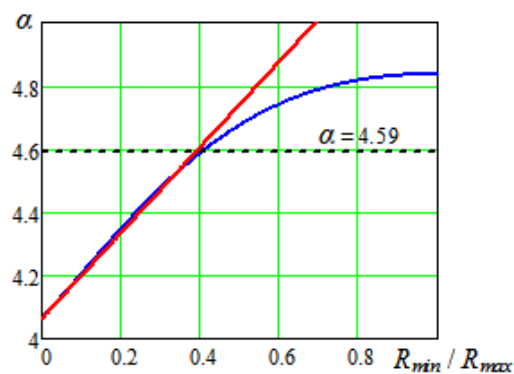

Figure 3. The dependence of the contact area ratio on the variation coefficient for the uniform distribution law.

Particularly, in the case of similar size of particles ($R_{min}/R_{max} \to 1$), $\alpha = 4.84$ as it was found above.

Thus, for the entire range of the ratio R_{min}/R_{max}, the contact area ratio α changes insignificantly in a range of 4.06–4.84. The exact bounds of this range are equal to $\alpha_{min} = 4\sqrt[3]{\pi/3} \approx 4.06$ for the widest range of particle size variation ($R_{min}/R_{max} \to 0$), and $\alpha_{max} = \sqrt[3]{36\pi} \approx 4.84$—for the narrowest range of particle size variation ($R_{min}/R_{max} \to 1$). Additionally, the integral mean value for the entire range of the ratio R_{min}/R_{max} is determined as follows:

$$\alpha = 4.06 \int_0^1 \frac{1 + \frac{R_{min}}{R_{max}} + \left(\frac{R_{min}}{R_{max}}\right)^2}{\left(1 + \frac{R_{min}}{R_{max}}\right)^{2/3}\left[1 + \left(\frac{R_{min}}{R_{max}}\right)^2\right]^{2/3}} d\left(\frac{R_{min}}{R_{max}}\right) = 4.59. \tag{17}$$

It should be noted that in the case of the presence of particles with a relatively wide range of changes in their size ($R_{min}/R_{max} < 0.4$), it is expedient to present the linearized expression for the contact area ratio. Applying the Maclaurin's series in terms of the first order of smallness with respect to the ratio R_{min}/R_{max}, the following can be obtained (Figure 3):

$$\alpha \approx 4.06\left(1 + \frac{1}{3}\frac{R_{min}}{R_{max}}\right). \tag{18}$$

Thus, for a relatively wide range of particle size variations ($R_{min}/R_{max} \to 0$), with enough accuracy for practical purposes, the contact area ratio equal to $\alpha = 4.59$ can be chosen.

4.2. Normal Distribution Law

In the case of the normal distribution law of the continuous random variable distribution of dispersed particles, the probability density is determined by the following formula [38]:

$$p(R) = \frac{a}{\sqrt{2\pi}\sigma}exp\left[-\frac{\left(R - R\right)^2}{2\sigma^2}\right], \tag{19}$$

where $\overline{R}$—the mathematical expectation of a continuous random variable as the mean radius of particles; σ—mean square deviation determined by the formula:

$$\sigma = \kappa R, \tag{20}$$

where κ—variation coefficient.

The normalizing factor a is introduced since the dispersed particle size varies in a range $[R_{min}, R_{max}]$ instead of traditional $[0, \infty)$.

Considering the dependence (11), the normalizing factor is determined as follows:

$$a = \frac{\sqrt{2\pi}\sigma}{\int_{R_{min}}^{R_{max}} exp\left[-\frac{(R-\overline{R})^2}{2\sigma^2}\right]dR}. \tag{21}$$

The substitution of this dependence on Equation (14) allows one to determine the contact area ratio. Due to the complexity of this dependence, it is expedient to use the three-sigma rule to determine a range of the most probable values of particle size with the quantile equal to 0.99:

$$\begin{aligned} R_{min} &= \overline{R} - 3\sigma = (1 - 3\kappa)\overline{R}; \\ R_{max} &= \overline{R} + 3\sigma = (1 + 3\kappa)\overline{R}. \end{aligned} \tag{22}$$

In this case, it can be shown that the expression for determining the contact area ratio does not depend on the particle size, but only on the variation coefficient. Additionally, up to the second-order smallness, it can be represented by the following analytical dependence:

$$\alpha \approx 4.84\left(1 - 0.52\kappa^{5/3}\right). \tag{23}$$

Particularly, in the case of similar size of particles ($\kappa \to 0$), $\alpha = 4.84$ as it was found above.

It should be noted that in the maximum range $[0, {}^1/_3]$ of changing the variation coefficient κ, the interfacial surface ratio α varies insignificantly in a range of 4.44–4.84. Moreover, the mean integral value for the entire range of this ratio (Figure 4) can be determined as follows:

$$\alpha = 3 \cdot 4.84 \int_0^{1/3}\left(1 - 0.52\kappa^{5/3}\right)d\kappa = 4.69. \tag{24}$$
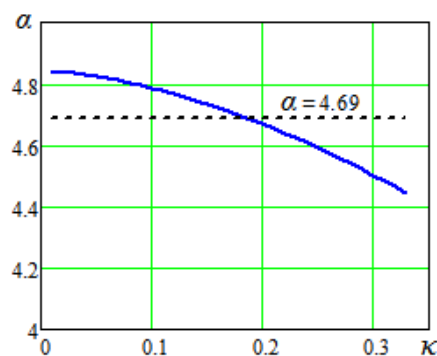

Figure 4. The dependence of the contact area ratio on the variation coefficient for the normal distribution law.

Thus, for enough accuracy for practical purposes, the contact area ratio can be chosen equal to its mean value $\alpha = 4.69$.

The comparison of the existing dependence for the specific interfacial surface with the proposed approach leads to introduce the correction factor *k*:

$$k = \sqrt{\frac{\alpha^3}{36\pi}}. \tag{25}$$

as a part of the following clarified expression:

$$a = k\frac{6c}{d_p}. \tag{26}$$

Particularly, for the case of uniform distribution of particle sizes, the minimum value of this coefficient is equal to $k = 4\sqrt{3}/9 \approx 0.77$. Additionally, for the case of the normal distribution of particle sizes, its minimum value is equal to $k = 0.88$.

As an example of calculation, determination of the interfacial surface between gaseous and liquid phases in the gas–liquid reactor with self-priming mixing device is presented for the following parameters: specific power $E = 2.8 \cdot 10^{-5}$ W/kg; average liquid flow rate $v_L = 4$ m/s; diameter and width of impeller $d_m = 0.105$ m and $b = 0.020$ m, respectively; coefficient of surface tension $\sigma = 0.073^3$ N/m; density of liquid and air $\rho_L = 1 \cdot 10^3$ kg/m^3 and $\rho_a = 1$ kg/m^3, respectively. The density of the gas–liquid mixture $\rho_m = \varphi\rho_a + (1 - \varphi)\rho_L$ is equal to 935 kg/m^3.

According to the practical recommendations for designing gas–liquid reactors, the average diameter of particles can be approximately evaluated as $d_p = 7.25 \cdot 10^{-3}\left(\frac{\sigma}{\rho_L}\right)^{0.6}E^{-0.4}$, which is equal to 1.58 mm. To evaluate a range of particle diameters according to the proposed methodology, the following parameters were used: height of the liquid layer under the impeller $h_p = 0.150$ m; acceleration of gravity $g = 9.81$ m/s^2; dynamic viscosity of liquid $\mu_L = 1 \cdot 10^{-3}$ Pa·s.

Experimental studies in a range of Reynolds numbers $Re = (3.2{-}7.5) \cdot 10^4$ have shown that the resistance coefficient of the mixing device $\zeta = 0.8$ is independent of Froude (*Fr*), Reynolds (*Re*), and homochronicity (*Ho*) numbers, but is the function of geometrical similarity simplexes only. For this case, a rotating frequency is evaluated by the expression $f = Re\frac{\mu_L}{\rho_L d_m^2}$, which is in a range of 3.2–7.5 Hz. However, its critical value $f_{cr} = \frac{1}{\pi d_m}\sqrt{\frac{2gh_p}{\zeta}}$ is equal to 5.8 Hz. Consequently, the average value of the operating frequency $f_{av} = (5.8 + 7.5)/2 = 5.4$ (Hz). In this case, the Froude number, which is determined as $Fr = \frac{f^2 d_m}{gh_p}$, varies in a range of 0.7–2.0. Consequently, considering the empirical coefficient $K = 0.28$, the gas volume fraction $\varphi = K\frac{b}{d_m}\frac{Fr_{max}-Fr_{min}}{1+K\frac{b}{d_m}(Fr_{max}-Fr_{min})}$ is equal to 0.07, and the interfacial surface $S = 8.2$ m^2.

As a result of the numerical calculations for the internal diameter of the apparatus $D = 0.325$ mm and the height of the mixture $H = 0.475$, the total volume $V = \frac{\pi D^2}{4}H$ is equal to 0.039 m^3. In this case, according to Equation (26), the average diameter of particles varies in a range of 1.4–1.9 mm, and the average value is equal to 1.65 mm, which corresponds to the previously evaluated parameter $d_p = 1.58$ mm with the relative error of about 4.5%.

5. Conclusions

Thus, a mathematical model for determining the interfacial surface during the separation process is proposed for the case of two-phase multicomponent systems with joint heat and mass transfer. As a result, a universal dependence (9) for determining the total surface of a heat and mass transfer is developed. It is proved that the total area of this surface depends on the volume of a medium and the volume concentration of the dispersed phase.

Based on the proposed probabilistic mathematical model, the dependence for determining a contact area ratio is proposed. The values of this ratio are determined for different laws of the distribution of dispersed particles. Particularly, for the case of the uniform distribution law, considering

all the possible range of size for dispersed particles, the contact area is in a range of 4.06–4.84, and its mean value is equal to 4.59. Additionally, in the case of normal distribution law, the contact area ratio is in a range of 4.44–4.84, and its mean value is equal to 4.69. The maximum value of this coefficient for all the distribution laws is equal to 4.84, and its averaged value varies insignificantly in a range of 4.59–4.69.

Moreover, the coefficient α for the uniform or normal distribution laws can be determined experimentally by comparing the dependence with the existing dimensionless criteria for the heat and mass exchange case studies using the proposed regression procedure.

The proposed approach allows one to clarify analytical dependencies for determining the interfacial surface during the mass-transfer processes in two-phase multicomponent systems considering the different fractional distribution of dispersed particles, which is valuable for ensuring the operating process in the corresponding technological equipment. As a result of the comparison of the existing dependence for the specific interfacial surface with the proposed approach, the correction factor was introduced. The minimum value of this factor varies in a range of 0.77–0.88 depending on the distribution law for dispersed particles.

Finally, the reliability of the developed model was proved on the example of the calculation of the interfacial surface in the gas–liquid reactor with a self-priming mixing device. As a result of numerical calculations, the relative error of determining the average size of dispersed particles is about 4.5%.

Author Contributions: Conceptualization, I.P., O.L., M.O. and V.I.; Formal analysis, I.P., V.S. (Vsevolod Sklabinskyi), V.S. (Vitaly Storozhenko,), Y.M. and J.P.; Investigation, O.L., V.S. (Vsevolod Sklabinskyi), V.S. (Vitaly Storozhenko,), M.O., V.I., O.S., S.W., A.K. and M.M.; Methodology, V.S. (Vsevolod Sklabinskyi), Y.M., V.I., J.P., O.S. and S.W.; Writing—original draft, I.P., O.L. and M.O. All authors have read and agreed to the published version of the manuscript.

Conflicts of Interest: The authors declare no conflict of interest.

References

1. Simion, D. *Calculation of the Effective Mass Transfer Area in Turbulent Contact Absorber*; Studia Universitatis Babes-Bolyai Chemia: Cluj-Napoca, Romania, 2016; Volume 61, pp. 227–238.
2. Kolev, N.; Nakov, S.; Ljutzkanov, L.; Kolev, D. Effective area of a highly efficient random packing. *Chem. Eng. Process.* **2006**, *45*, 429–436. [CrossRef]
3. Yang, K.; Chu, G.; Zou, H.; Sun, B.; Shao, L.; Chen, J.F. Determination of the effective interfacial area in rotating packed bed. *Chem. Eng. J.* **2011**, *168*, 1377–1382. [CrossRef]
4. Liu, Y.; Gu, Y.; Xu, C.; Qi, G.; Jiao, W. Mass transfer characteristics in a rotating packed bed with split packing. *Chin. J. Chem. Eng.* **2015**, *23*, 868–872. [CrossRef]
5. Luo, Y.; Luo, J.Z.; Chu, G.W.; Zhao, Z.Q.; Arowo, M.; Chen, J.F. Investigation of effective interfacial area in a rotating packed bed with structured stainless steel wire mesh packing. *Chem. Eng. Sci.* **2017**, *170*, 347–354. [CrossRef]
6. Luo, Y.; Chu, G.W.; Zou, H.K.; Zhao, Z.Q.; Dudukovic, M.P.; Chen, J.F. Gas-liquid effective interfacial area in a rotating packed bed. *Ind. Eng. Chem. Res.* **2012**, *51*, 16320–16325. [CrossRef]
7. Tsai, C.Y.; Chen, Y.S. Effective interfacial area and liquid-side mass transfer coefficients in a rotating bed equipped with baffles. *Sep. Purif. Technol.* **2015**, *144*, 139–145. [CrossRef]
8. Lyu, Y.; Brusseau, M.; Ouni, E.A.; Araujo, J.B.; Su, X. The gas-absorption/chemical-reaction method for measuring air-water interfacial area in natural porous media. *Water Resour. Res.* **2017**, *53*, 9519–9527. [CrossRef]
9. Brusseau, M.L.; Narter, M.; Schnaar, G.; Marble, J. Measurement and estimation of organic-liquid/water interfacial areas for several natural porous media. *Environ. Sci. Technol.* **2009**, *43*, 3619–3625. [CrossRef]

10. Brusseau, M.L.; Peng, S.; Schnaar, G.; Murao, A. Measuring air-water interfacial areas with X-ray microtomography and interfacial partitioning tracer tests. *Environ. Sci. Technol.* **2007**, *41*, 1956–1961. [CrossRef]

11. Costanza-Robinson, M.S.; Harrold, K.H.; Lieb-Lappen, R.M. X-ray microtomography determination of air-water interfacial area-water saturation relationships in sandy porous media. *Environ. Sci. Technol.* **2008**, *42*, 2949–2956. [CrossRef]

12. McDonald, K.; Carroll, K.C.; Brusseau, M.L. Comparison of fluid-fluid interfacial areas measured with X-ray microtomography and interfacial partitioning tracer tests for the same samples. *Water Resour. Res.* **2016**, *52*, 5393–5399. [CrossRef] [PubMed]

13. Shi, S.Y.; Xu, J.Y. Flow field of continuous phase in a vane-type pipe oil-water separator. *Exp. Therm. Fluid Sci.* **2015**, *60*, 208–212. [CrossRef]

14. Liu, L.; Zhao, L.; Yang, X.; Wang, Y.; Xu, B.; Liang, B. Innovative design and study of an oil-water coupling separation magnetic hydrocyclone. *Sep. Purif. Technol.* **2018**, *213*, 389–400. [CrossRef]

15. Liaposhchenko, O.; Pavlenko, I.; Ivanov, V.; Demianenko, M.; Starynskyi, O.; Kuric, I.; Khukhryanskiy, O. Improvement of parameters for the multi-functional oil-gas separator of "Heater-Treater" type. In Proceedings of the 2019 IEEE 6th International Conference on Industrial Engineering and Applications (ICIEA), Tokyo, Japan, 12–15 April 2019; pp. 66–71.

16. Fesenko, A.; Basova, Y.; Ivanov, V.; Ivanova, M.; Yevsiukova, F.; Gasanov, M. Increasing of equipment efficiency by intensification of technological processes. *Period. Polytech. Mech. Eng.* **2019**, *63*, 67–73. [CrossRef]

17. Petinrin, M.O.; Dare, A.A. Numerical investigation of the concave-cut baffles effect in shell-and-tube heat exchanger. *J. Eng. Sci.* **2019**, *6*, 1–9. [CrossRef]

18. Liaposhchenko, O.; Pavlenko, I.; Demianenko, M.; Starynskyi, O.; Pitel, J. The methodology of numerical simulations of separation process in SPR-separator. *CEUR Workshop Proc.* **2019**, *2353*, 822–832.

19. Cao, C.; Cheng, J. A novel Cu(OH)2 coated filter paper with superhydrophobicity for the efficient separation of water-in-oil emulsions. *Mater. Lett.* **2018**, *217*, 5–8. [CrossRef]

20. Lu, H.; Yang, Q.; Xu, X.; Wang, H.L. Effect of the mixed oleophilic fibrous coalescer geometry and the operating conditions on oily wastewater separation. *Chem. Eng. Technol.* **2016**, *39*, 255–262. [CrossRef]

21. Li, F.; Wang, Z.; Huang, S.; Pan, Y.; Zhao, X. Flexible, durable, and unconditioned superoleophobic/superhydrophilic surfaces for controllable transport and oil-water separation. *Adv. Funct. Mater.* **2018**, *28*, 1706867. [CrossRef]

22. Pylypaka, S.; Klendiy, M.; Zaharova, T. Movement of the particle on the external surface of the cylinder, which makes the translational oscillations in horizontal planes. In *Advances in Design, Simulation and Manufacturing*; DSMIE 2018. Lecture Notes in Mechanical Engineering; Springer: Cham, Switzerland, 2019; pp. 336–345. [CrossRef]

23. Sriram, S.; Kumar, A. Separation of oil-water via porous PMMA/SiO2 nanoparticles superhydrophobic surface. *Colloids Surf. A Physicochem. Eng. Asp.* **2018**, *563*, 271–279. [CrossRef]

24. Liang, Y.; Kim, S.; Kallem, P.; Choi, H. Capillary effect in Janus electrospun nanofiber membrane for oil/water emulsion separation. *Chemosphere* **2019**, *221*, 479–485. [CrossRef] [PubMed]

25. Esfahani, M.R.; Aktij, S.A.; Dabaghian, Z.; Firouzjaei, M.D.; Rahimpour, A.; Eke, J.; Escobar, I.C.; Abolhassani, M.; Greenlee, L.F.; Esfahani, A.R.; et al. Nanocomposite membranes for water separation and purification: Fabrication, modification, and applications. *Sep. Purif. Technol.* **2018**, *213*, 465–499. [CrossRef]

26. Afarani, H.T.; Sadeghi, M.; Moheb, A.; Esfahani, E.N. Optimization of the gas separation performance of polyurethane-zeolite 3A and ZSM-5 mixed matrix membranes using response surface methodology. *Chin. J. Chem. Eng.* **2018**, *27*, 110–129. [CrossRef]

27. Chakrabarty, B.; Ghoshal, A.K.; Purkait, M.K. Ultrafiltration of stable oil-in-water emulsion by polysulfone membrane. *J. Membr. Sci.* **2008**, *325*, 427–437. [CrossRef]

28. Liaposhchenko, O.; Pavlenko, I.; Monkova, K.; Demianenko, M.; Starynskyi, O. Numerical simulation of aeroelastic interaction between gas-liquid flow and deformable elements in modular separation devices. In *Advances in Design, Simulation and Manufacturing II*; DSMIE 2019. Lecture Notes in Mechanical Engineering; Springer: Cham, Switzerland, 2020; pp. 765–774. [CrossRef]

29. Liaposhchenko, O.O.; Sklabinskyi, V.I.; Zavialov, V.L.; Pavlenko, I.V.; Nastenko, O.V.; Demianenko, M.M. Appliance of inertial gas-dynamic separation of gas-dispersion flows in the curvilinear convergent-divergent channels for compressor equipment reliability improvement. *IOP Conf. Ser. Mater. Sci. Eng.* **2017**, *233*, 012025. [CrossRef]

30. Wen, J.; Sun, Q.; Sun, Z.; Gu, H. An improved image processing technique for determination of volume and surface area of rising bubble. *Int. J. Multiph. Flow* **2018**, *104*, 294–306. [CrossRef]

31. Lu, J.; Corvalan, C.M.; Chew, Y.M.J.; Huang, J.Y. Coalescence of small bubbles with surfactants. *Chem. Eng. Sci.* **2018**, *196*, 493–500. [CrossRef]

32. Chen, Y.; Lian, Y. Numerical investigation of coalescence-induced self-propelled behavior of droplets on non-wetting surfaces. *Phys. Fluids* **2018**, *30*, 112102. [CrossRef]

33. Plyatsuk, L.D.; Ablieieva, I.Y.; Vaskin, R.A.; Yeskendirov, M.; Hurets, L.L. Mathematical modeling of gas-cleaning equipment with a highly developed phase contact surface. *J. Eng. Sci.* **2018**, *5*, 19–24. [CrossRef]

34. Ochowiak, M.; Wlodarczak, S.; Pavlenko, I.; Janecki, D.; Krupinska, A.; Markowska, M. Study on interfacial surface in modified spray tower. *Processes* **2019**, *7*, 532. [CrossRef]

35. Sklabinskyi, V.; Liaposhchenko, O.; Pavlenko, I.; Lytvynenko, O.; Demianenko, M. Modelling of liquid's distribution and migration in the fibrous filter layer in the process of inertial-filtering separation. In *Advances in Design, Simulation and Manufacturing*; DSMIE 2018. Lecture Notes in Mechanical Engineering; Springer: Cham, Switzerland, 2019; pp. 489–497. [CrossRef]

36. Liaposchenko, O.; Pavlenko, I.; Nastenko, O. The model of crossed movement and gas-liquid flow interaction with captured liquid film in the inertial-filtering separation channels. *Sep. Purif. Technol.* **2017**, *173*, 240–243. [CrossRef]

37. Garrick, S.C.; Buhlmann, M. Fundamentals of gas-to-particle mass transfer. In *Modeling of Gas-to-Particle Mass Transfer in Turbulent Flows*; Springer Briefs in Applied Sciences and Technology; Springer: Cham, Switzerland, 2018; pp. 1–16. [CrossRef]

38. Tarasevych, Y.; Sovenko, N.; Savchenko, I. Influence of the stochastic nature parameters of throttle channels on characteristic of automatic balancing device of the centrifugal pump. In *Advances in Design, Simulation and Manufacturing*; DSMIE 2018. Lecture Notes in Mechanical Engineering; Springer: Cham, Switzerland, 2019; pp. 374–381. [CrossRef]